Available online at www.sciencedirect.com
SCIENCE DIRECT®
Journal of Power Sources 143 (2005) 236–242
JOURNAL OF POWER SOURCES
www.elsevier.com/locate/jpowsour

0.6 Ah Li/V_2O_5 battery prototypes based on solvent-free PEO–$LiN(SO_2CF_2CF_3)_2$ polymer electrolytes

G.B. Appetecchi, J.H. Shin, F. Alessandrini, S. Passerini*

Ente Per le Nuove Tecnologie, I'Energia e l'Ambiente, IDROCOMB Centro Ricerche Casaccia, Via Anguillarese 301, Rome 00060, Italy

Received 22 June 2004; received in revised form 4 November 2004; accepted 15 November 2004
Available online 24 January 2005

Abstract

The cycling performance of all-solid-state, scaled-up, 0.6 Ah Li/V_2O_5 polymer battery prototypes, realized within a National Project devoted to development of electric vehicles, is presented and discussed. Poly(ethyleneoxide)–$LiN(SO_2CF_2CF_3)_2$ (PEO–LiBETI) films were used as electrolyte separators. The prototypes, formed by parallel stacking ten single bipolar cells, were assembled by the direct lamination of the components, namely, lithium foil anodes, PEO–LiBETI electrolyte films and composite V_2O_5-based cathode films. The performance of the Li/PEO–LiBETI/V_2O_5 prototypes, scaled-up from single cells, was evaluated in terms of specific capacity, energy and cycle life at different discharge current densities. The results have indicated high reproducibility of the manufacturing process and the feasibility to large scale-up the all-solid-state, lithium polymer batteries based on solvent-free prepared PEO–LiBETI electrolyte.

Keywords: PEO; LiBETI; Lithium polymer battery; Solvent-free electrolyte; Hot-pressing; Composite cathode

1. Introduction

Rechargeable, lithium polymer batteries, LPB, represent an excellent choice as electrochemical power sources characterized by high energy density, good cyclability and safety [1–4]. The poly(ethylene oxide)–lithium salt, PEO–LiX, complexes are promising candidates as electrolytes for LPB applications [5–9]. Large research efforts have been devoted to the development of PEO electrolyte formulations capable to combine high conductivity, good interfacial stability with lithium metal anode, and good mechanical properties [10–13]. A common approach is the use of a lithium salt having a very large counter-ion, which is able to interfere with the crystallization process of the polymer chains [14,15], thereby, promoting amorphous regions and increasing the lithium ion transport in the polymer electrolyte [6,15,16].

Following the latter approach, we have shown that the use of a large anion ($N(SO_2CF_2CF_3)_2^-$, BETI) lithium salt enhances the conductivity of PEO-based polymer electrolytes [17]. In addition, PEO–LiBETI polymer electrolytes develop a very stable interface with lithium metal anode both under rest conditions and current flow [18]. Tests performed on cells, containing crystalline V_2O_5-based cathodes have shown very good performance of PEO–LiBETI polymer electrolytes for EV application at medium-high temperatures [19]. No additional capacity fading due to the interaction of the polymer electrolyte with the electrodes was detected.

In this scenario, we decided to investigate the scale-up of the Li/V_2O_5 polymer cells based on solvent-free PEO–LiBETI electrolyte to realize prototypes having a capacity ranging from 0.5 to 1 Ah. Vanadium pentoxide was selected as active material because of its commercial availability. Very large amounts of cathode components (10–20 kg) were needed for the realization of the cathode tapes that were produced on the high-volume production line by Ferrania

* Corresponding author. Tel.: +39 06 3048 4985; fax: +39 06 3048 6357.
E-mail address: passerini@casaccia.enea.it (S. Passerini).

0378-7753/$ – see front matter © 2004 Elsevier B.V. All rights reserved.
doi:10.1016/j.jpowsour.2004.11.039

S.p.A. No other 3 V cathode materials were commercially available.

In this work, we report the characteristics and the cycling performance of all-solid-state, rechargeable, 0.6 Ah Li/V_2O_5 prototypes, formed by stacking ten bipolar cells connected in parallel.

2. Experimental

2.1. PEO–LiBETI electrolyte membranes

PEO–LiBETI polymer electrolyte films with an EO/Li molar ratio of 20 [17] were prepared by a completely dry, solvent-free procedure developed at ENEA [12,13,17]. Briefly, the components PEO ($M_w = 4 \times 10^6$, Polyox WSR301, Union Carbide) and LiBETI (3M) were dried under vacuum at 50 and 150 °C, respectively, for at least 24 h before use. The materials were sieved, gently mixed by ball-milling in the appropriate ratio and then extruded or hot-pressed at 100 °C to form thin tapes. The latter were cold-calendered down to a thickness of 80–90 μm. The whole procedure was carried out in a controlled atmosphere dry-room having a relative humidity (RH) lower than 0.1% (Corridi s.r.l.).

2.2. V_2O_5 composite cathodes

The composite cathodes were prepared by following a procedure developed at ENEA and industrially scaled-up by Ferrania S.p.A. Basically, the process involved the deposition of slurry onto both faces of an aluminum foil current collector (battery grade, 25 μm thick) by doctor-blade technique to obtain bipolar cathode tapes. The slurry has the following dry composition: V_2O_5 (Pechiney) active material 60 wt.%, carbon (Super-P, MMM carbon) electronic conductor 10 wt.%, PEG (Carbowax, DOW formerly Union Carbide) 27 wt.%, PEO (Polyox WSR301, DOW, formerly Union Carbide) 3 wt.%. A chloromethane/methanol mixture (2:1 in weight) with traces of acetone was used as solvent that was allowed to evaporate under a hood. Then the coated films were dried under vacuum at 50 °C for 48 h. The absence of salt in the composite cathode favored the moisture and solvent removal. At the end of the process, the thickness of the bipolar composite cathode tapes (including the aluminum substrate) was about 180 μm with an apparent density (mass/volume) of about 1.5 g cm^{-3}, corresponding to an active material (V_2O_5) surface area loading of 6.4 mg cm^{-2}, approximately.

2.3. Li/V_2O_5 prototypes

Scaled-up Li/PEO–LiBETI/V_2O_5 battery prototypes were realized by stacking ten bipolar cells (connected in parallel). The cell design, outlined by the sequence *Li/SPE/Cathode/SPE/Li*, is illustrated in Fig. 1. The sizes of the cathode tape (5.2 cm × 3.0 cm) and the lithium anode (5.2 cm × 3.0 cm) were slightly lower than the polymer electrolyte layer (5.8 cm × 3.4 cm) to prevent accidental short-circuit. The cathode substrate (aluminum, 25 μm thick) was also used as the current collector, while a copper foil (25 μm thick) was used as the anodic current collector. The assembly of prototypes firstly involved the realization of anodic *SPE/Li/SPE* half-cells. The latter were fabricated by hot-laminating (about 100 °C) a lithium foil (50 μm thick) between two polymer electrolyte layers. Then, the half-cells were alternatively overlapped to the cathode tapes following the sequence:

$$Li/SPE/Cathode/SPE/(Li/SPE/Cathode/SPE)_9/Li.$$

The final stacks (5.8 cm × 3.4 cm × 0.4 cm), composed of 10 cathode tapes, 11 lithium foils and 20 polymer electrolyte layers, were housed in coffee-bag envelopes, which were evacuated under vacuum for 45–60 min before sealing to minimize the O_2 and N_2 content [12] and to ensure a good contact between the electrodes and the polymer electrolytes.

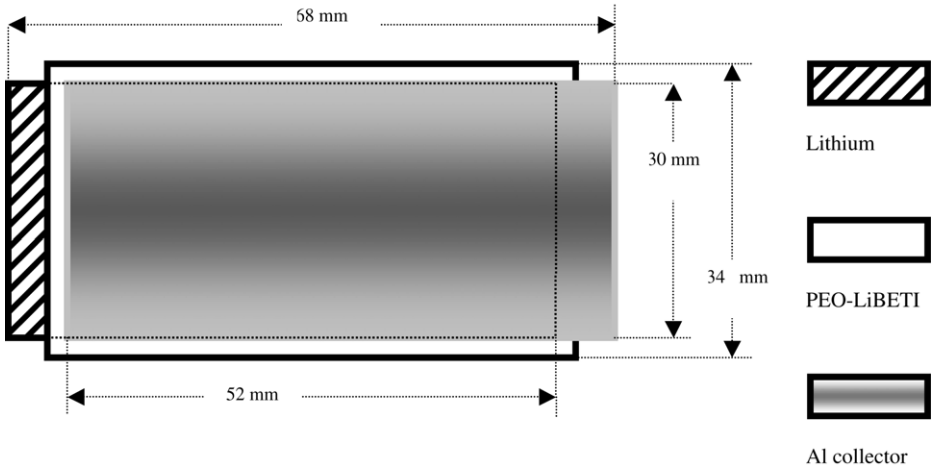

Fig. 1. Cell design of the single Li/SPE/Cathode/SPE/Li bipolar cell.

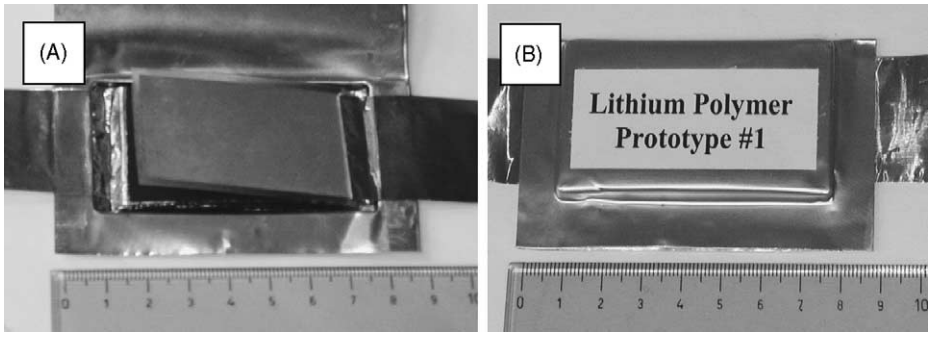

Fig. 2. Pictures of a scaled-up, 0.6 Ah class, Li/PEO–LiBETI/V_2O_5 battery prototype upon housing in coffee-bag envelope (panel A) and sealing under vacuum (panel B), respectively.

The weight of the final device was about 13 g, including the current collectors and the package. The assembly as well as the electrochemical tests of prototypes was carried out in a controlled atmosphere dry-room (RH < 0.1%, Corridi s.r.l.). Fig. 2 shows pictures of a Li/V_2O_5 polymer battery prototype after housing in coffee-bag envelope (panel A) and sealing under vacuum (panel B), respectively.

Since the composite cathodes did not contain the lithium salt the final EO/Li molar ratio was fixed by the relative amount of the salt-containing PEO in the electrolyte and the salt-free PEO in the cathode. The final EO/Li ratio was about 25, which falls in a flat region of the conductivity versus salt concentration curve at operating temperatures higher than 60 °C [17]. The prototypes were cathode-limited (anode/cathode capacity ratio of about 3).

The characteristics of the scaled-up Li/PEO–LiBETI/V_2O_5 battery prototypes are summarized in Table 1. The batteries exhibit a reversible capacity of 0.59 Ah, considering the V_2O_5 specific capacity equal to 0.295 Ah g^{-1} (two equivalent of Li per mole of V_2O_5) at an average discharge voltage of 2.7 V. This corresponds to a theoretical specific energy of the prototypes equal to 145 Wh kg^{-1} not including the weight of package or 122 Wh kg^{-1} for the whole prototypes. These values are subjected to a substantial improvement upon further optimization of the weight of the components. For instance, large production volumes would make metal foils of appropriate thickness for the cathode substrate and the current collectors easily available. The thickness of the electrolyte layers could be reduced from 80–90 μm to 40–50 μm by using industrial extrusion-blowing equipment. The size of the electrolyte layers, cathode tabs, current collectors and packaging could be reduced by using a specialized assembly line. In Table 2, are reported the size and weight of the components of the Li/PEO–LiBETI/V_2O_5 battery prototype. With the optimizations cited above the weight of the device would be lowered to 7.8 g with a corresponding gravimetrical energy exceeding 200 Wh kg^{-1}.

Table 1
Characteristics of the Li/PEO–LiBETI/V_2O_5 battery prototypes

Single cells (#)	10
Size (cm)	6.8 × 3.4 × 0.4
Active surface area (cm^2)	312
Weight (g)	13 (11[a])
Reversible capacity (Ah)[b]	0.59
Specific energy (Wh kg^{-1})	122 (145[a])

[a] Weight of package not included.
[b] V_2O_5 specific capacity equal to 295 Ah g^{-1} (two equivalent of Li per mole of V_2O_5).

2.4. Electrochemical tests

Impedance measurements were performed using a Solartron Instruments 1260 Impedance Analyzer coupled with a Solartron Electrochemical Interface 1287 at 20 and 90 °C.

Table 2
Size, total weight and weight fraction of the components of the Li/PEO–LiBETI/V_2O_5 battery prototypes reported in this work and upon further optimization

	Present prototype			Optimized prototype		
	$L \times H \times T$ (mm)	Weight (g)	Weight fraction (wt.%)	$L \times H \times T$ (mm)	Weight (g)	Weight fraction (wt.%)
Lithium anodes	60 × 30 × 0.05	0.6	4.6	58 × 30 × 0.05	0.58	7.4
Polymer electrolyte separators	56 × 34 × 0.09	6.0	46.1	56 × 34 × 0.04	2.7	34.6
Cathodes	52 × 30 × 0.14	2.4	18.5	52 × 30 × 0.14	2.4	30.8
Cathode substrates (Al)	60 × 30 × 0.03	1.5	11.5	60 × 30 × 0.02	1.0	12.8
Anode current collector (Cu)	45 × 30 × 0.025	0.32	2.4	15 × 30 × 0.025	0.11	1.4
Cathode current collector (Al)	45 × 30 × 0.05	0.18	1.4	15 × 30 × 0.025	0.03	0.4
Package	Overall area 112 cm^2	2.0	15.5	Overall area 55 cm^2	0.98	12.6
Battery Prototype	68 × 34 × 4	13.0	100.0	68 × 34 × 3	7.8	100.0
Specific energy (Wh g^{-1})	–	122	–	–	204	–

The AC tests were carried out after selected charge/discharge cycles in the 5 kHz–0.1 Hz frequency range.

The cycling tests were performed by means of a Maccor S4000 battery tester in the 2.0–3.6 V range at discharge current densities ranging from 0.050 to 2.0 mA cm^{-2}. The performance of the batteries was evaluated in terms of capacity, energy and cycle life at 90 °C. The temperature of the batteries was set by placing them in forced ventilation ovens. Before the measurements, the batteries were left to thermally equilibrate as well as to allow the diffusion of the lithium salt inside the cathodes.

3. Results and discussion

Fig. 3 reports the AC responses of a scaled-up, 0.6 Ah Li/PEO–LiBETI/V_2O_5 battery prototype at 20 °C (panel A) and 90 °C (panel B). A semicircle, associated with interfacial resistance [22], is followed by an inclined straight line towards the real axes, Z', that is related to the diffusive electrolyte contribute [22]. The intercept of the semicircle with the real axes gives the PEO membrane ionic resistance [22]. At 20 °C the pristine prototype exhibits an overall resistance of about 75 Ω. Upon assembly, the battery was kept at 90 °C for 72 h and then cooled down to 20 °C. No relevant decay of the electrolyte resistance (about 30 Ω) was observed, while the interfacial resistance decreased from 45 to 30 Ω, thus indicating the optimization of the polymer electrolyte/electrode interface. At 90 °C (panel B) a remarkable but expected decrease of the battery impedance to about 0.5 Ω is observed.

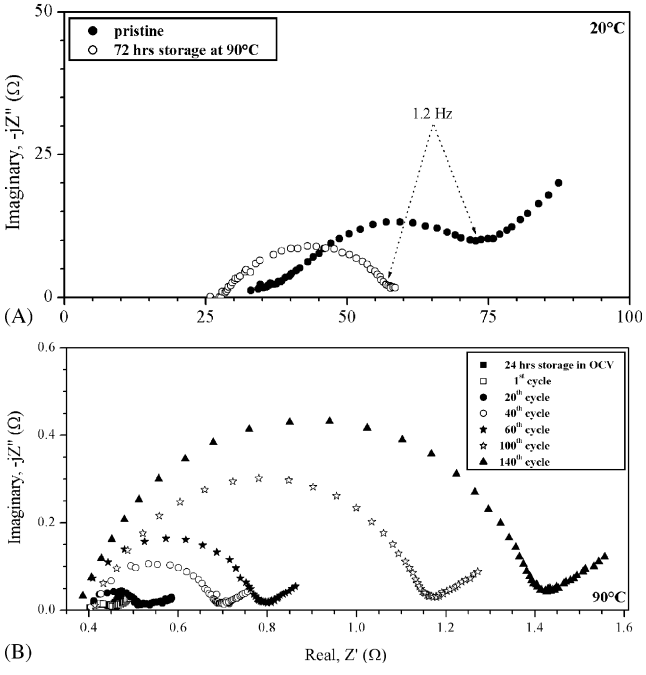

Fig. 3. AC responses of a scaled-up, 0.6 Ah class, Li/PEO–LiBETI/V_2O_5 battery prototype at 20 °C (panel A) and 90 °C (panel B) after selected charge/discharge cycles (see legend). Frequency range: 5 kHz–0.1 Hz.

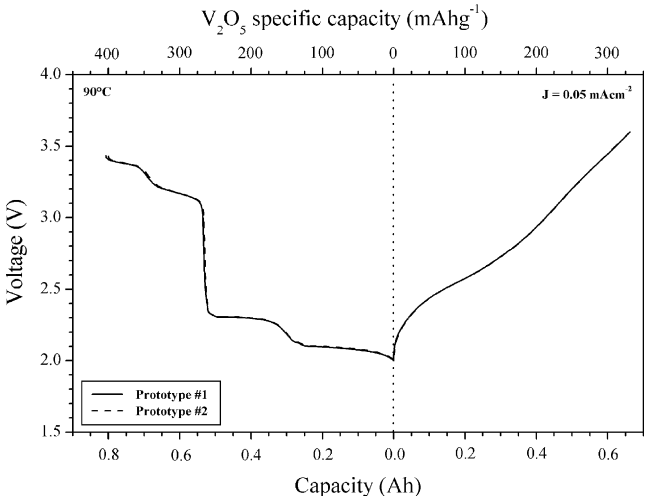

Fig. 4. Voltage/capacity profile of two scaled-up, 0.6 Ah class, Li/PEO–LiBETI/V_2O_5 battery prototypes held at 90 °C during the first discharge/charge cycle. Current density: 0.05 mA cm^{-2}.

In particular, the interfacial resistance decreased to a value lower than 0.05 Ω. This would correspond to an ohmic drop lower than 80 mV at a current density equal to 0.5 mA cm^{-2} (C/3.7). However, a relevant increase of the prototype interfacial resistance is observed during prolonged charge/discharge cycles (panel B). This is most likely due to the spontaneous degradation of the V_2O_5 active material on cycling that exhibits a sharp electronic conductivity decay in passing from crystalline to amorphous structure [20,21], thus strongly increasing the charge transfer resistance.

In Fig. 4, is plotted the voltage versus capacity profile of two Li/PEO–LiBETI/V_2O_5 battery prototypes held at 90 °C during the first discharge/charge cycle. The current density was set to 0.05 mA cm^{-2} corresponding to a C/20 discharge rate. As expected from a crystalline V_2O_5-based cathode, the first discharge showed a series of plateau related to the lithium insertion in specific intercalation sites [20,21]. About 2.75 equivalent of Li per mole of V_2O_5 were intercalated in the initial discharge down to 2.0 V, corresponding to a capacity of 0.8 Ah. Such a large lithium insertion caused the full disruption of the crystalline structure [21], as indicated by the smooth voltage profile during the following charge. In this step, 82% of the lithium inserted (0.66 Ah) was recovered, most likely due to the moderate anodic cut-off voltage fixed at 3.6 V to prevent polymer electrolyte oxidation [23]. The Li/V_2O_5 polymer batteries displayed practically overlapping voltage profiles, which indicates for the high reproducibility of the scale-up manufacturing process developed.

Fig. 5 illustrates consecutive discharge curves of a Li/PEO–LiBETI/V_2O_5 battery prototype held at 90 °C at various current densities (see legend). The charge current density was fixed to 0.2 mA cm^{-2} (C/9.3 rate). Apart from a modest capacity reduction, no substantial feature change was observed from 0.1 mA cm^{-2} (C/18.6) to 0.5 mA cm^{-2} (C/3.7). The delivered capacity decreased about 14% from 0.58 Ah (C/18.6) to 0.5 Ah (C/3.7) for a current increase factor of 5.

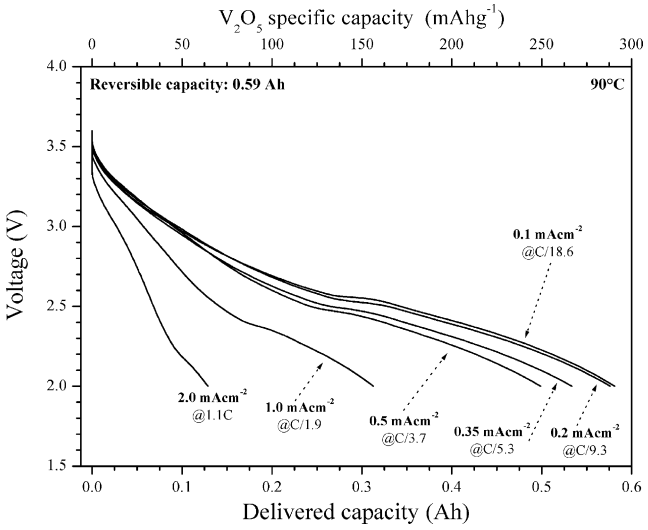

Fig. 5. Voltage/discharge capacity profiles of a scaled-up, 0.6 Ah class, Li/PEO–LiBETI/V_2O_5 battery prototype held at 90 °C during consecutive cycles at different discharge current densities (see legend). The discharge rates are also reported. Charge current density: 0.2 mA cm^{-2}.

This is of particular interest since EV applications require discharge times close to 3 h. In addition, the ohmic drop was lower than 100 mV in the 0.1–0.5 mA cm^{-2} range. The prototypes are still capable to deliver more than 52% (0.31 Ah) and 22% (0.13 Ah) of the reversible capacity at 1.0 mA cm^{-2} (C/1.9) and 2.0 mA cm^{-2} (1.1C), respectively.

The delivered capacity versus discharge current density dependence for two scaled-up Li/PEO–LiBETI/V_2O_5 prototypes held at 90 °C is reported in Fig. 6. The charge current density was fixed to 0.2 mA cm^{-2}. Also, the capacity versus discharge current density behavior of two single bipolar cells is shown for comparison. Once more, the results supports for the high reproducibility of the manufacturing process of the scaled-up Li/V_2O_5 prototypes. The data plotted in Fig. 6 show two well-defined trends with a knee at 0.5 mA cm^{-2}

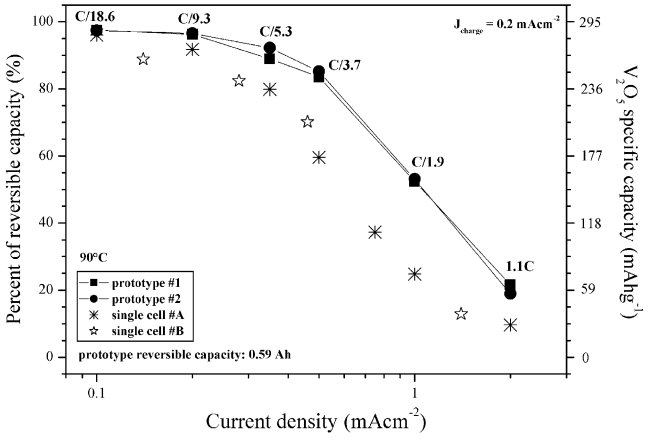

Fig. 6. Delivered capacity, reported as percent of reversible capacity, vs. current density plot of two single Li/PEO–LiBETI/V_2O_5 bipolar cells and two scaled-up, 0.6 Ah class, battery prototypes held at 90 °C. The discharge rates are also reported. Charge current density: 0.2 mA cm^{-2}.

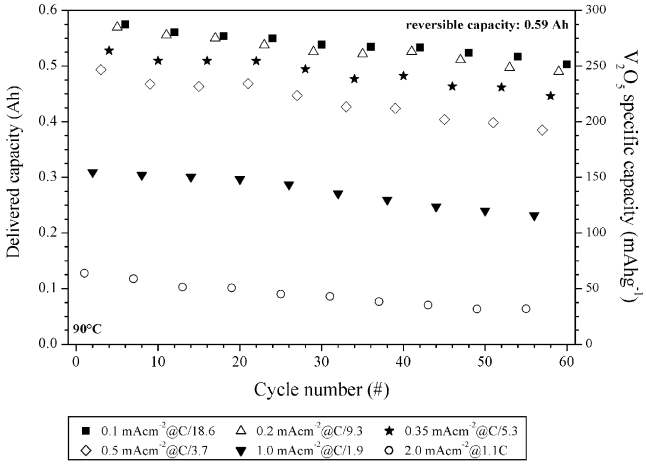

Fig. 7. Delivered capacity vs. cycle number behavior of a scaled-up, 0.6 Ah class, Li/PEO–LiBETI/V_2O_5 battery prototype during consecutive cycles at different discharge current densities (see legend). The discharge rates are also reported. Charge current density: 0.2 mA cm^{-2}. T = 90 °C.

(C/5.3), due to the delivered capacity limitation originating from different diffusive phenomena taking place in the electrolyte (higher rates) and in the active material phase (lower rates). The prototypes are capable to deliver almost the full capacity (>85%) up to 0.5 mA cm^{-2} (C/3.7). The results clearly show that the scaled-up Li/V_2O_5 prototypes perform better than the single bipolar cells, especially at medium-high rates, i.e., >0.35 mA cm^{-2} @C/5. This indicates the feasibility to scale-up all-solid-state Li/V_2O_5 cells based on PEO–LiBETI polymer electrolyte.

The rate performance is also observed in Fig. 7 where is displayed the delivered capacity versus cycle trend at decreasing discharge current densities from 2.0 mA cm^{-2} (1.1C) to 0.1 mA cm^{-2} (C/18/6). The charge current density was always 0.2 mA cm^{-2} (C/9.3). The scaled-up Li/V_2O_5 prototypes showed good performance upon prolonged cycling tests. Upon 55 consecutive cycles the prototypes delivered about 0.49 Ah, 0.39 Ah and 0.064 Ah at 0.2 mA cm^{-2} (C/9.3), 0.5 mA cm^{-2} (C/3.7) and 2.0 mA cm^{-2} (1.1C), respectively, corresponding to 83, 66 and 11% of the reversible capacity. No relevant effect on the capacity fading due to the discharge rate was observed up to a 0.5 mA cm^{-2} current density. The observed fading of about 0.3% per cycle, corresponds to the intrinsic fading of deeply discharged crystalline V_2O_5-based cathodes [20,23]. The performance decay is to be associated with the intrinsic capacity fading of V_2O_5 rather than to PEO–LiBETI polymer electrolyte misbehavior and/or cell design.

Fig. 8 illustrates the cycling behavior of a Li/PEO–LiBETI/V_2O_5 battery prototype cycled in the voltage range from 2.0 to 3.6 V. The charge current was fixed to 0.35 mA cm^{-2} (C/5.3), while the discharge process was driven at 0.5 mA cm^{-2} (C/3.7). The results are reported in terms of voltage/discharge capacity profile of selected charge/discharge cycles (panel A) and of capacity versus cycle plot (panel B). From the shape of the curves, it looks

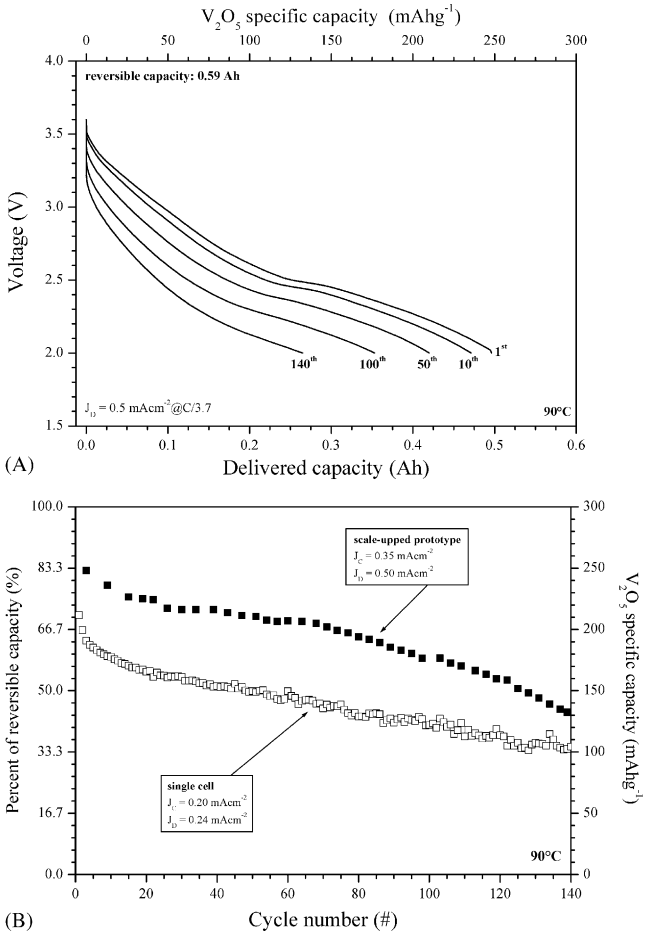

Fig. 8. Voltage/capacity profile (panel A) of selected discharge processes and cycling performance (panel B) of a scaled-up, 0.6 Ah class, Li/PEO–LiBETI/V_2O_5 battery prototype held at 90 °C. Charge current density: 0.35 mA cm^{-2} (C/5.3). Discharge current density: 0.5 mA cm^{-2} (C/3.7). The cycling behavior of a single Li/V_2O_5 cell (data extracted from reference [19]) is reported in panel B for comparison.

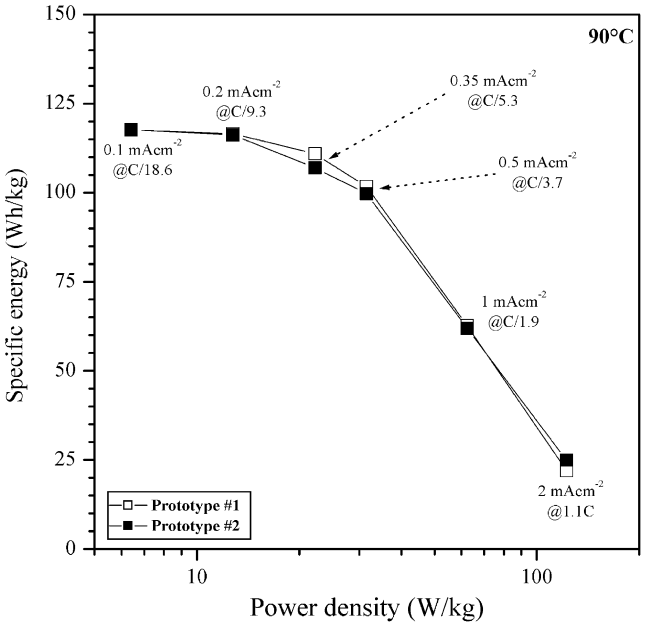

Fig. 9. Ragone plot of two scaled-up, 0.6 Ah class, Li/PEO–LiBETI/V_2O_5 battery prototypes held at 90 °C. The discharge rates and current densities are also reported. The energy and power density values are calculated taking into account the total weight of the prototypes, i.e., including the weight of the current collectors and packaging.

like there are two causes for the performance decay: (i) initial voltage drop related to the increased charge transfer resistance at the polymer electrolyte/cathode interface; (ii) disappearance of the plateau around 2.5 V. The prototype delivered an initial capacity of about 0.5 Ah that decayed to 0.264 Ah upon 140 charge/discharge cycles with a fade of 0.3% per cycle. Once more, this indicates that the capacity fading is associated to the cathode failure rather than to polymer electrolyte faults. Panel B also illustrate the cycling behavior of two single Li/V_2O_5 cells for comparison. The data, extracted from reference [19], are referred to charge/discharge processes driven at lower current densities than for the prototypes. Once more, the scaled-up prototypes showed better performance than the single cells, especially at medium-high rates, i.e., >0.35 mA cm^{-2} @C/5.

Fig. 9 illustrates the Ragone plot of two scaled-up Li/PEO–LiBETI/V_2O_5 battery prototypes held at 90 °C. The discharge rates and current densities are also reported. The energy and power density values are calculated taking into account the total weight of the scaled-up prototypes, i.e., including the weight of the current collectors and the package. Once more, the devices exhibited very similar performance. At low rates (<0.2 mA cm^{-2} i.e., C/9.3) the prototypes delivered a specific energy close to 120 Wh kg^{-1}, i.e., in good agreement with the theoretical value, with a power density of 6.4 W kg^{-1}. At high rates (2.0 mA cm^{-2} @1.1C), the energy value falls down to 22 Wh kg^{-1}, while the power density increases up to 122 Wh kg^{-1}.

4. Conclusions

Rechargeable Li/V_2O_5 cells based on lithium-conducting PEO–LiBETI polymer films were scaled-up to fabricate all-solid-state, 0.6 Ah class, prototypes for EV applications. The prototypes delivered initial reversible capacity and specific energy equal to 0.58 Ah and 120 Wh kg^{-1}, respectively, in excellent agreement with the theoretical values. At C/3.7 rate (0.5 mA cm^{-2}) the prototypes were still capable to deliver about 85% of the reversible capacity. The prototypes were affected by a capacity fading that corresponds to the intrinsic one of V_2O_5-based cathodes. The results showed that the scaled-up prototypes outperformed the single cells previously developed. This evidenced the validity of the lithium polymer battery design and processing developed by ENEA and the reproducibility of the manufacturing process, thus demonstrating the feasibility to scale-up Li/PEO–LiBETI/V_2O_5 cells to realize all-solid-state batteries.

Acknowledgement

Financial contribution from MIUR (Ministero per l'lstruzione, l'Universita e la Ricerca) is kindly acknowledged. The authors thank Dr. Boyd of 3M for kindly providing the LiBETI salt. Ferrania S.p.A. is acknowledged.

References

[1] B. Scrosati, Nature 373 (1995) 557.
[2] S.P. Beaton, G.A. Bishop, Y. Ziang, L.L. Ashbaugh, D.R. Lawson, D.H. Stedman, Science 268 (1995) 991.
[3] J. Aragane, K. Matsui, H. Andoh, S. Sukuki, H. Fukuda, H. Ikeaya, K. Kitaba, R. Ishikawa, J. Power Sources 68 (1997) 13.
[4] F.R. Kalhammer, A. Kozawa, C.B. Moyer, B.B. Owens, Electrochem. Soc. Interface 5 (1996) 32.
[5] M. Armand, J.M. Chabagno, M.J. Duclot, in: P. Vashishita, J.N. Mundy, G.K. Shenoy (Eds.), Fast Ion Transport in Solid, Elsevier, New York, 1989.
[6] F.M. Gray, Polymer Electrolytes, Royal Society of Chemistry Monographs, Cambridge, 1997.
[7] F.M. Gray, M. Armand, in: T. Osaka, M. Datta (Eds.), Energy Storage System for Electronics, Gordon and Breach, Amsterdam, 2000.
[8] P. Lightfoot, M.A. Metha, P.G. Bruce, Science 262 (1993) 883.
[9] C.A. Vincent, B. Scrosati, Modern Batteries. An Introduction to Electrochemical Power Sources, second ed., Arnold, London, 1993.
[10] W. Wieczorek, K. Such, H. Wycislik, J. Plocharski, Solid State Ionics 36 (1989) 225.
[11] M.C. Borghini, M. Mastragostino, S. Passerini, B. Scrosati, J. Electrochem. Soc. 142 (1995) 2118.
[12] G.B. Appetecchi, S. Scaccia, S. Passerini, J. Electrochem. Soc. 147 (2000) 4448.
[13] G.B. Appetecchi, F. Alessandrini, R.G. Duan, A. Arzu, S. Passerini, J. Power Sources 1 (2001) 4335.
[14] V. Rossi Albertini, G.B. Appetecchi, R. Caminiti, F. Cillocco, F. Croce, C. Sadun, J. Macromol. Sci. Phys. B36 (1997) 629.
[15] S. Lascaud, M. Perrier, A. Valle, C. Besner, J. Prud'homme, M. Armand, Macromolecules 27 (1994) 7469.
[16] G. Feuillade, P. Perche, J. Appl. Electrochem. 5 (1975) 63.
[17] G.B. Appetecchi, W. Henderson, P. Villano, M. Berrettoni, S. Passerini, J. Electrochem. Soc. 148 (2001) 1171.
[18] G.B. Appetecchi, S. Passerini, Electrochem. Acta 45 (2000) 2139.
[19] P. Villano, M. Carewska, G.B. Appetecchi, S. Passerini, J. Electrochem. Soc. 149 (2002) A1282.
[20] C. Delmas, H. Cognac-Aradou, J. Power Sources 54 (1995) 406.
[21] J. Scarminio, A. Talledo, A.A. Andersson, S. Passerini, F. Decker, Electrochem. Acta 38 (1993) 1637.
[22] J.R. Macdonald, Impedance Spectroscopy, John Wiley & Sons, New York, 1987.
[23] P.P. Prosini, S. Passerini, R. Vellone, W.H. Smyrl, J. Power Sources 75 (1998) 73.